

IONIC CONCENTRATION CHANGES IN THE TUBULAR SYSTEM OF RAT VENTRICULAR CARDIAC CELL MODEL

M. Pásek¹, G. Christé², J. Šimurda³

Summary: We present a design of a model of rat ventricular cardiomyocyte with transverse-axial tubular system and the results of the first simulations of tubular ionic concentration changes at different stimulation rates. The morphology of tubular system and the distribution of ionic channels in tubular membrane were described to meet the recent data of Soeller and Cannell (1999) and of Orchard's group in Leeds. Exploration of activity-dependent changes in tubular ionic concentrations revealed an increase in relative Ca^{2+} depletion from 7.3 % to 14 % when increasing the stimulation frequency from 1 Hz to 5 Hz. Meanwhile, relative K^+ accumulation decreased from 4.3 % to 3 %. These effects led to a limitation of intracellular Ca^{2+} overload.

1. Introduction

In our previous work (Pásek et al. 2002; 2003), we introduced development of a model of cardiac ventricular cell electrical activity including quantitative description of transverse - axial tubular system (TATS). The model reproduced general features of mammalian ventricular cardiac cells ignoring differences observed in different species (guinea pig, rat, dog, rabbit, human etc). The preliminary simulations predicted that TATS is a place of significant concentration changes (depletion of tubular calcium ions by more than 12 % and accumulation of tubular potassium ions by more than 4 % at 1 Hz stimulation rate) with implications for cellular electrical activity and intracellular ionic homeostasis.

In the next steps we decided to design new improved ventricular cell models that would respect the known significant interspecies differences in both TATS morphological features and the distribution of ion transfer mechanisms.

In this paper, we introduce development of a model of rat ventricular cell. Quantitative description of TATS is based on recent microscopic analysis of rat ventricular cell ultrastructure (Soeller and Cannel, 1999; Satoh et al., 1996) and on data from measurements of sarcolemmal ionic currents before and after formamide-induced detubulation obtained by the group of Prof. Orchard at the School of Biomedical Sciences of University of Leeds (Brette et al. 2002, Yang et al. 2002). The model was used for quantitative exploration of ionic concentration changes in TATS of rat ventricular myocyte.

¹ Ing. Michal Pásek, Ph.D.: Institute of Thermomechanics, Czech Academy of Science - branch Brno; Technická 2; 616 69 Brno; Czech Republic; e-mail: pasek@umtn.fme.vutbr.cz

² Dr. Georges Christé.: INSERM E0219, DRDC/DVE, CENG F-38054, Grenoble; CEDEX 9; France

³ Doc. RNDr. Jiří Šimurda CSc.: Institute of Physiology of Masaryk University, Komenského nám. 2; Brno; Czech Republic

2. Development of model of rat ventricular myocyte

The mathematical model of Pandit et al. (2001) was used as a basis for design of the present model of rat ventricular cell with TATS. The model includes formulation of the ion transporting systems in surface and tubular membrane, description of the sarcoplasmic reticulum (uptake and release compartment), Ca^{2+} -buffers and subsarcolemmal compartment-fuzzy space. A schematic diagram of the model is shown in Fig. 1.

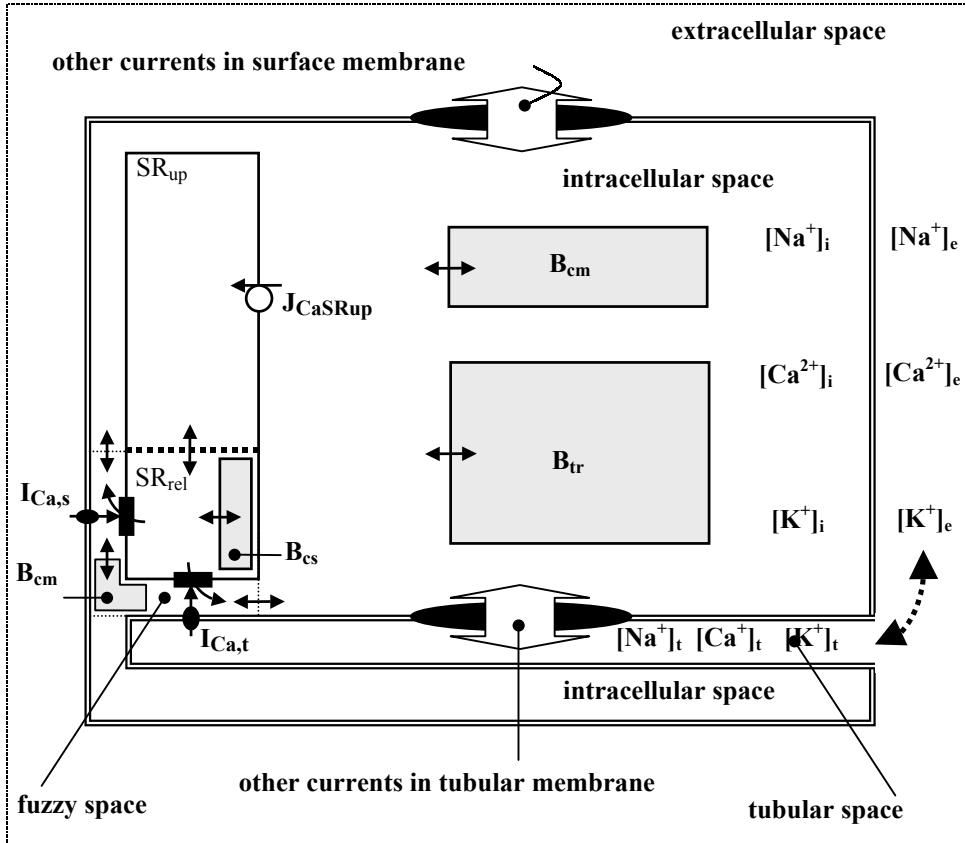


Figure 1. Schematic diagram of the model of rat ventricular cell. The description of electrical activity of surface (s) and tubular (t) membrane comprises following ionic currents: fast sodium current (I_{Na}), calcium current through L-type channels (I_{Ca}), transient outward potassium current (I_{Kto}), steady-state outward potassium current (I_{Kss}), inward rectifying potassium current (I_{K1}), hyperpolarization-activated current (I_f), background currents (I_{Cab} , I_{Nab} , I_{Kb}), sodium-calcium exchange current (I_{NaCa}), sodium-potassium pump current (I_{NaK}), and calcium pump current (I_{pCa}). The intracellular space contains a fuzzy space, Ca^{2+} -uptake and Ca^{2+} -release compartments of sarcoplasmic reticulum (SR_{up} , SR_{rel}) and Ca^{2+} -buffers calmodulin (B_{cm}), troponin (B_{tr}) and calsequestrin (B_{cs}). The small filled rectangles in SR_{rel} membrane represent ryanodine receptors. The small bi-directional arrows denote Ca^{2+} diffusion between intracellular compartments. Ionic diffusion between tubular and bulk space is represented by the dashed arrow.

The modifications of the model introduced by Pandit et al. (2001) and incorporation of TATS are described in the following sections:

Modification of membrane transport system

■ The description of I_{Na} -channel gating was restricted to three-activation (m^3) and one inactivation (h) gates. The rate constants for activation (α_m, β_m) and inactivation (α_h, β_h) were formulated according to experimental data of Brown et al. (1981). Their resulting forms are:

$$\alpha_m = 117,26 \cdot (V_m + 59,3) / (1 - \exp(-0,55 \cdot (V_m + 59,3))),$$

$$\beta_m = 3800 \cdot \exp(-0,0723 \cdot (V_m + 61)),$$

$$\alpha_h = 15,518 / (1 + \exp(0,188 \cdot (V_m + 68,2))),$$

$$\beta_h = 18,77 \cdot (V_m + 64,4) / (1 - \exp(-0,4 \cdot (V_m + 64,4))).$$

■ To achieve realistic value of reversal voltage for I_{Na} , 12 % of channel permeability was assigned to potassium ions (Nordin (1993)).

■ The constant term (0.017) in the description of the voltage dependent time constants of fast and slow I_{Ca} -channel inactivation was omitted to comply more precisely with experimental data of Katsube et al. 1998. The modified formulas are:

$$\tau_{f1} = 0.105 \cdot \exp(-((V_m + 45)/12)^2) + 0.04 / (1 + \exp(-(V_m + 25)/25)) + 0.015 / (1 + \exp((V_m + 75)/25)),$$

$$\tau_{f2} = 0.041 \cdot \exp(-((V_m + 47)/12)^2) + 0.08 / (1 + \exp(-(V_m + 55)/5)) + 0.015 / (1 + \exp((V_m + 75)/25)).$$

■ The description of I_{K1} was corrected to be consistent with experimental data from rat myocytes:

$$I_{K1} = g_{K1} \cdot (V_m - E_K - 1.7) / (1 + \exp(1.613 \cdot F / (R \cdot T) \cdot (V_m - E_K - 1.7))) \cdot (1.0 + \exp((K_e - 0.9988) / -0.124)).$$

■ The total membrane maximum conductivity of background calcium current and the maximum current density of calcium pump were set to values $0.648 \mu\text{S}/\text{cm}^2$ and $1 \mu\text{A}/\text{cm}^2$ to ensure realistic levels of diastolic intracellular Ca^{2+} at different frequencies (Frampton et al., 1991).

■ The stimulus current was incorporated into the equation controlling the intracellular potassium concentration to comply with the charge conservation principle (Hund et al., 2001).

■ The maximum specific conductivity and current density of individual ion transfer mechanisms in surface membrane ($g_{Xmax,s}, I_{Xmax,s}$) and in tubular membrane ($g_{Xmax,t}, I_{Xmax,t}$) were computed according to the relations:

$$g_{Xmax,s} = g_{Xmax} \cdot (1 - f_{X,t}) \cdot (S_{m,s} + S_{m,t}) / S_{m,s},$$

$$g_{Xmax,t} = g_{Xmax} \cdot f_{X,t} \cdot (S_{m,s} + S_{m,t}) / S_{m,t},$$

$$I_{Xmax,s} = I_{Xmax} \cdot (1 - f_{X,t}) \cdot (S_{m,s} + S_{m,t}) / S_{m,s},$$

$$I_{Xmax,t} = I_{Xmax} \cdot f_{X,t} \cdot (S_{m,s} + S_{m,t}) / S_{m,t},$$

where $g_{X,max}$ and $I_{X,max}$ denote the maximum specific conductivity and current density related to 1 cm² of total membrane (adopted from Pandit et al. 2001). $f_{X,t}$ denote fractions of individual currents flowing through tubular membrane. Their numeric values (Tab. 1) were obtained within the framework of our collaboration with the laboratory of Prof. Clive Orchard at the School of Biomedical Sciences of the University in Leeds. $S_{m,s}$ and $S_{m,t}$ stand for the area of peripheral and tubular membrane, respectively.

	$f_{X,t}$		$g_{X,max}, I_{X,max}$
I_{Na}	56 % *	$g_{Na,max}$	8 mS/cm ²
I_{Ca}	87 %	$g_{Ca,max}$	0.34 mS/cm ²
I_{Kto}	56 % *	$g_{Kto,max}$	0.35 mS/cm ²
I_{Kss}	76 %	$g_{Kss,max}$	0.07 mS/cm ²
I_{K1}	56 % *	$g_{K1,max}$	0.24 mS/cm ²
I_f	56 % *	$g_{f,max}$	0.015 mS/cm ²
$I_{Na,b}$	56 % *	$g_{Na,b,max}$	0.802 μ S/cm ²
$I_{Ca,b}$	56 % *	$g_{Ca,b,max}$	0.648 μ S/cm ²
$I_{K,b}$	56 % *	$g_{K,b,max}$	1.380 μ S/cm ²
k_{NaCa}	81 %	$k_{NaCa,max}$	0.1 nA/cm ² /mM ⁴
I_{NaK}	59 %	$I_{NaK,max}$	0.8 μ A/cm ²
I_{pCa}	56 % *	$I_{pCa,max}$	1 μ A/cm ²

Table 1. Electrical properties of membrane transport system in the model. The values of the parameter $f_{X,t}$ denoting fractions of membrane currents flowing through tubular membrane were obtained from the laboratory of Prof. Orchard at the University in Leeds. Asterisks indicate data determined under assumption of uniform density of corresponding transporters in peripheral and tubular membrane. The symbols $g_{X,max}$ and $I_{X,max}$ represent the maximum specific conductivity and current density related to 1 cm² of total membrane as proposed by Pandit et al. (2001) (the values of $g_{Ca,b,max}$ and $I_{pCa,max}$ were changed).

Modification of intracellular Ca²⁺ handling

In their model Pandit et al. (2001) adopted description of intracellular Ca²⁺- handling from a quantitative model of canine midmyocardial ventricular cell (Winslow et al., 1999) that exhibits significant differences from the behaviour of rat ventricular cell in particular when higher stimulation rates are applied. To simulate dynamic changes of intracellular Ca²⁺ as observed in rat cardiomyocytes (Frampton et al., 1991), some model parameters had to be changed: increase of Ca²⁺-ATPase forward rate parameter of sarcoplasmic reticulum to value 0.4 mM/s, increase of time constant for Ca²⁺-transfer from SR_{up} to SR_{rel} compartment to value 20 ms and decrease of time constant for Ca²⁺-transfer between fuzzy space and cytoplasm to 8 ms.

Electrical interaction between surface and tubular membrane

According to our previous models (Pásek et al., 2002; 2003) the TATS was described as a single compartment separated from the surface membrane by the mean resistance of the tubular system (R_{st}) connected to the bulk pericellular solution. The contribution of one tubule to R_{st} was expressed as the resistance of a cylindrical conductor whose length, radius and

specific resistivity corresponded to one half of the tubular effective length ($l_t/2$), its average radius (r_t), and the specific resistivity of the extracellular solution (ρ_{ext}), respectively. (For the Tyrode solution, $\rho_{ext} \approx 83.33 \Omega \text{ cm.}$) Taking into account that, from the electric point of view, the TATS represents a parallel combination of all (n_t) tubules in the model cell, the mean resistance of the tubular system can be calculated from the relation

$$R_{st} = \rho_{ext} l_t / (2 \pi r_t^2 n_t).$$

As follows from the electrical equivalent scheme in Fig. 2, the stimulating current I_m equals the sum of the sarcolemmal current I_{ms} and the current through the TATS I_{mt} :

$$I_m = I_{ms} + I_{mt}.$$

In current clamp conditions $I_m = 0$ throughout except for the duration of the short (1 ms) suprathreshold stimuli. It follows that a common current

$$I_{circ} = I_{ms} = -I_{mt} = (V_{ms} - V_{mt}) / R_{st}$$

circulates through both membrane systems.

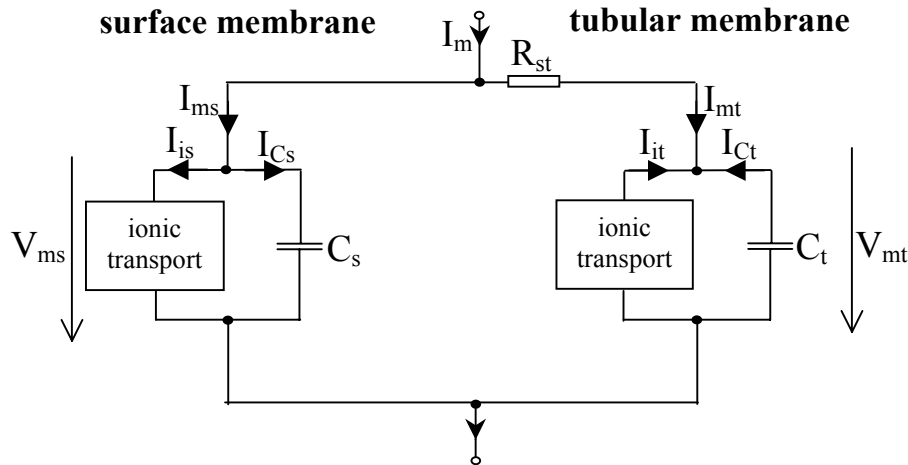


Figure 2. Electrical interaction between the surface and tubular membrane. V_s , I_{is} , I_{cs} , C_s and V_t , I_{it} , I_{ct} , C_t are, respectively, membrane voltage, total ionic current, capacitive current and membrane capacity of the surface and tubular membranes. R_{st} is the mean luminal resistance of the TATS.

Ionic diffusion between tubular and extracellular space

The time constants of ionic diffusion between the TATS and the extracellular space were set to 470 ms for calcium ions and 150 ms for potassium and sodium ions to meet the results of measurements published by Yao et al. (1997).

Myocyte ultrastructure

The geometric parameters of the TATS were set to comply with the results of microscopic analysis in rat ventricular myocytes (Soeller and Cannell 1999; Satoh et al., 1996): fractional volume of TATS ($\sim 3.6\%$), ratio TATS-area/cellular volume ($0.44 \mu\text{m}^2/\mu\text{m}^3$), ratio total membrane area/cellular volume ($0.68 - 0.89 \mu\text{m}^2/\mu\text{m}^3$), tubular diameter ($0.2 - 0.3 \mu\text{m}$) and

spacing of tubular mouth in peripheral membrane ($\sim 1.8 \mu\text{m}$). They comprise density of tubule mouths in the surface membrane ($0.3 \text{ tubules}/\mu\text{m}^2$), diameter of the tubules ($d_t = 0.3 \mu\text{m}$) and their mean length ($l_t = 4.5 \mu\text{m}$). Applying these parameters and the above ratios in the model with total membrane area $10000 \mu\text{m}^2$, the peripheral membrane represents $4495 \mu\text{m}^2$ (44.95 pF), the tubular membrane $5605 \mu\text{m}^2$ (56.05 pF), the cellular volume $12739 \mu\text{m}^3$ and the tubular volume $420.38 \mu\text{m}^3$. The fractional volumes of intracellular compartments (SR_{up} , SR_{rel} and fuzzy space) were set according to Pandit et al. (2001).

3. Results

Figures 3 and 4 illustrate the basic behaviour of the model at the stimulation rate of 5 Hz that is within the range of values of the resting heart rates reported for rat at rest (Vornanen, 1992). Fig. 3 depicts steady state electrical responses of surface and tubular membrane to stimulation pulses of magnitude 4.5 nA and of duration 1 ms. Included are action potentials (V_m), main ionic currents underlying depolarization (I_{Na} , I_{Ca}), repolarization (I_{Kto} , I_{Kss} , I_{K1}) and carrier mediated currents (I_{NaK} , I_{NaCa}) in both membrane systems.

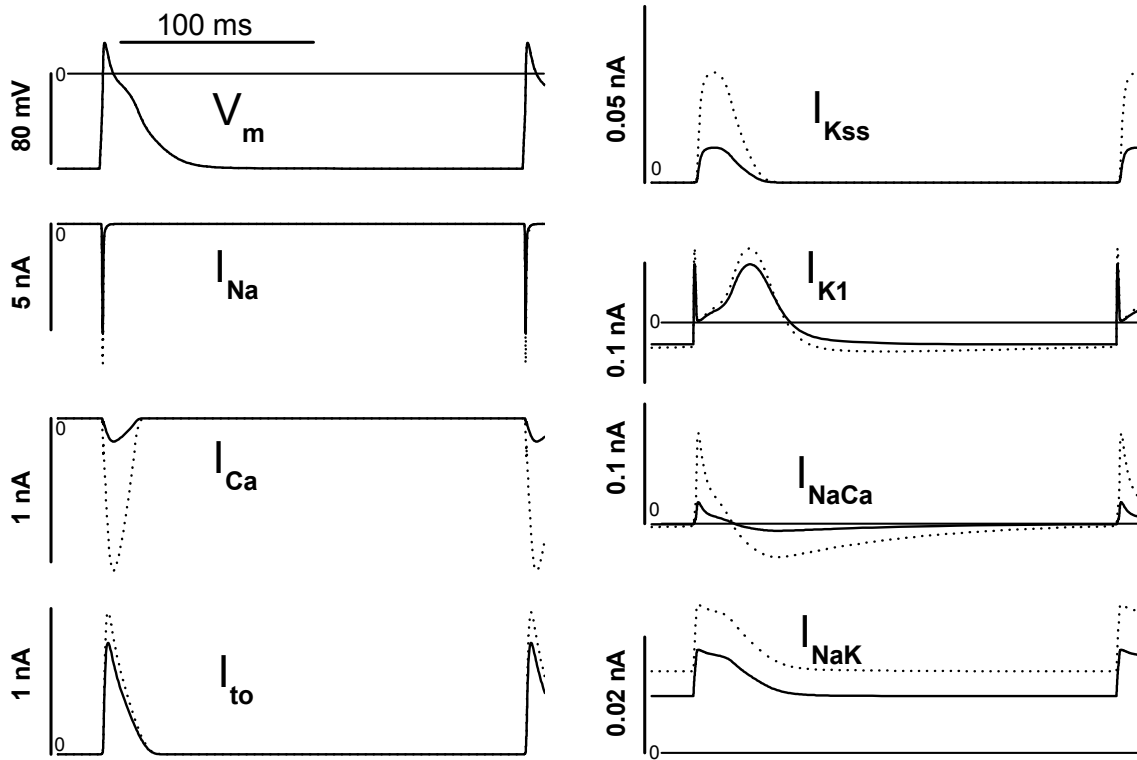


Figure 3. Action potentials (V_m) and main ionic currents (I_{Na} , I_{Ca} , I_{Kto} , I_{Kss} , I_{K1} , I_{NaCa} , I_{NaK}) in surface (solid lines) and tubular (dotted lines) membrane in response to stimulation pulses (4.5 nA, 1 ms) applied at frequency of 5 Hz. The differences between APs of both membrane systems are negligible. The striking differences between the magnitudes of corresponding currents in surface (solid lines) and tubular (dotted lines) membrane result from different area of tubular membrane versus surface membrane as well as from unequal fractions of transporters localised in each of the two membrane systems (see Table 1).

Fig. 4 depicts the changes of ionic concentrations in the sarcoplasmic reticulum, cytoplasm and TATS accompanying the electrical responses in Fig. 3. The transient increase in $[Ca^{2+}]_i$ from diastolic level (270 nmol/l) to systolic level (1.29 μ mol/l) occurs early after the onset of AP and reflects the rapid release of Ca^{2+} from the release compartment of sarcoplasmic reticulum (SR_{rel}). It is mirrored as a fall of $[Ca^{2+}]_{SRrel}$ from 1.55 mmol/l to 0.63 mmol/l. The subsequent decline of $[Ca^{2+}]_i$ caused by concurrent Ca^{2+} uptake into the uptake compartment of sarcoplasmic reticulum (SR_{up}) and calcium extrusion by the Na/Ca exchanger and sarcolemmal Ca^{2+} -pump (I_{pCa}) is considerably modulated by intracellular Ca^{2+} buffers (troponin and calmodulin). The steady state relative changes of $[Na^+]_i$ and $[K^+]_i$ are low but the end-diastolic levels of these concentrations exhibit a substantial shift from the values at rest ($[Na^+]_{i,rest} = 5.08$ mmol/l, $[K^+]_{i,rest} = 140$ mmol/l and $[Ca^{2+}]_{i,rest} = 31$ nmol/l, not shown).

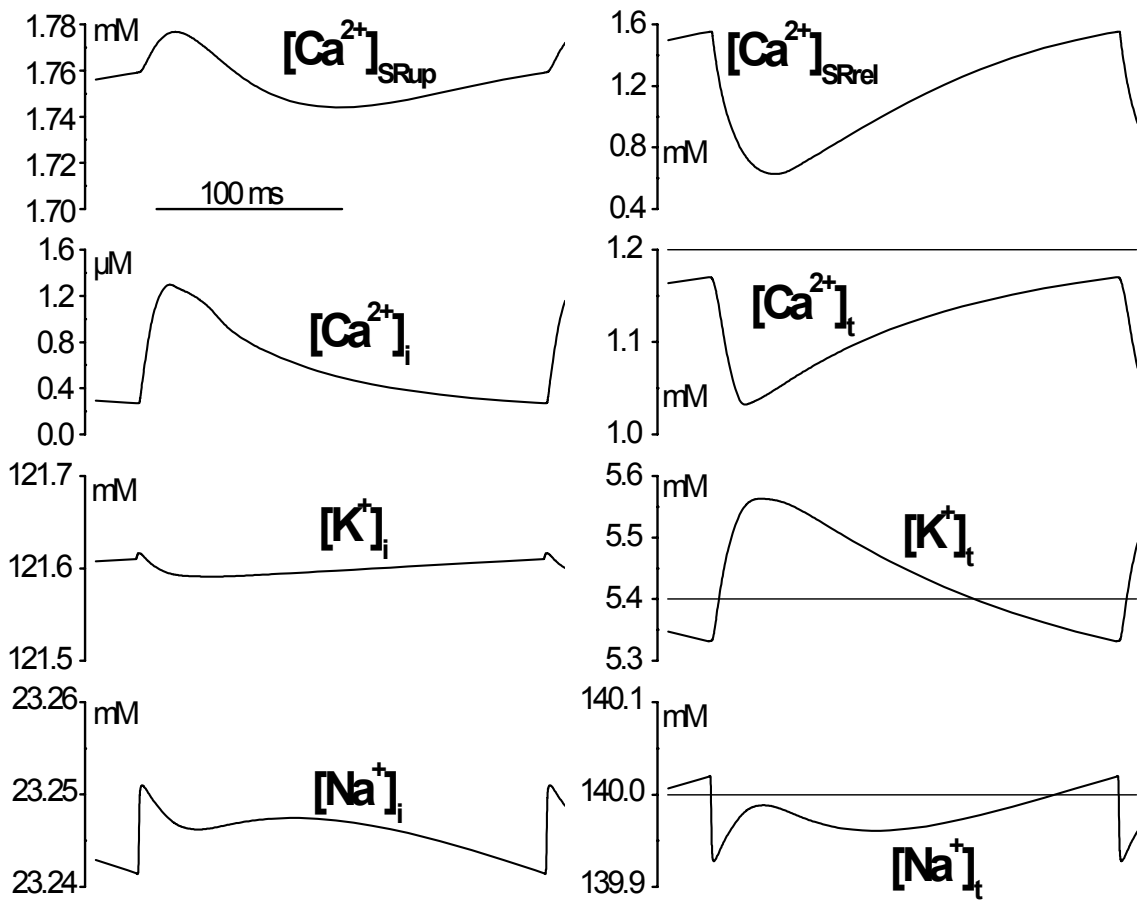


Figure 4. Concentration changes of Ca^{2+} in uptake and release compartments of sarcoplasmic reticulum ($[Ca^{2+}]_{SRup}$, $[Ca^{2+}]_{SRrel}$), and of Ca^{2+} , K^+ , Na^+ in myoplasm ($[Ca^{2+}]_i$, $[Na^+]_i$, $[K^+]_i$) and TATS ($[Ca^{2+}]_t$, $[Na^+]_t$, $[K^+]_t$). Steady state simulation at 5 Hz. Horizontal lines represent bulk extracellular concentration levels for Ca^{2+} , K^+ and Na^+ ions.

When explored at different stimulation rates. The depletion of tubular calcium increased with the increase of stimulation frequency (Fig. 5) and amounted 7.3 %, 9 % and 14 % for 1 Hz, 3 Hz and 5 Hz, respectively. On the contrary, the accumulation of tubular potassium

decreased with increasing stimulation frequency and amounted 4.3 %, 3.3 % and 3 % for 1 Hz, 3 Hz and 5 Hz, respectively. The relative changes of tubular sodium concentration appeared to be negligible.

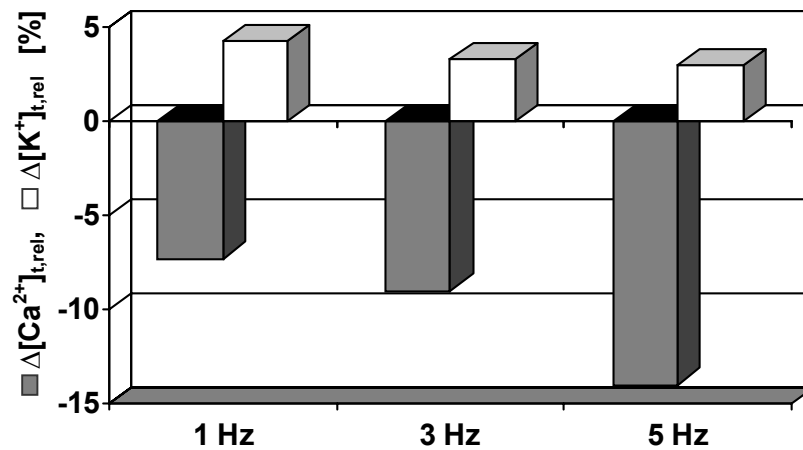


Figure 5. Rate dependence of relative changes of calcium and potassium concentration in TATS.

4. Conclusion

The present model is the first one to explore the effect of ionic concentration changes in TATS on electrical activity of rat ventricular cardiac cells. A dynamically stable state was reached at a physiological rate of activity (5 Hz) in which intracellular and tubular concentrations are kept far from their equilibrium values for the system at rest. A significant transient depletion of Ca^{2+} ions (14 %) and transient accumulation of K^+ ions (4 %) in the tubular system were present and exhibited a limitation of intracellular Ca^{2+} overload. A detailed exploration of physiological consequences of this phenomenon is the subject of our next work.

5. Acknowledgments

This study was supported by the grant 204/02/D129 from the Grant Agency of the Czech Republic, by project AVOZ 2076919 from the Institute of Thermomechanics of Czech Academy of Sciences and by the project J07/98:141100004 from the Ministry of Education, Youth and Sports of the Czech Republic.

6. References

- Brette, F., Komukai, K., Orchard, C.H. (2002) Validation of formamide as a detubulation agent in isolated rat cardiac cells. *Am. J. Physiol. Heart. Circ. Physiol.*, 283, pp. H1720-H1728.
- Brown, A.M., Lee, K. S., Powell, T. (1981) Sodium current in single rat heart muscle cells. *J. Physiol.*, 318, pp. 479-500.

- Frampton, J.E., Orchard, C.H., Boyett, M.R. (1991) Diastolic, systolic and sarcoplasmic reticulum [Ca^{2+}] during inotropic interventions in isolated rat myocytes. *J. Physiol.*, 437, pp. 351-375.
- Hund J.H., Kucera J.P., Otani N.F. and Rudy Y. (2001) Ionic charge conservation and long-term steady state in the Luo-Rudy dynamic cell model. *Biophys. J.*, 81, pp. 3324-3331.
- Katsube, Y., Yokoshiki, H., Nguyen, L., Yamamoto, M., Sperelakis, N. (1998) L-type Ca^{2+} currents in ventricular myocytes from neonatal and adult rats. *Can. J. Physiol. Pharmacol.*, 76, pp. 873-881.
- Nordin, C. (1993) Computer model of membrane current and intracellular Ca^{2+} flux in the isolated guinea pig ventricular myocyte. *Am. J. Physiol.*, 265, pp. H2117-H2136.
- Pandit S.V., Clark, R.B, Giles, W.R., Demir, S.S. (2001) A mathematical model of action potential heterogeneity in adult rat left ventricular myocytes. *Biophys. J.*, 81, pp 3029-3051.
- Pásek, M., Christé, G., Šimurda, J. (2002) Quantitative modelling of effect of transverse-axial tubular system on electrical activity of cardiac cells: development of model, in: *CD of the Conference Engineering Mechanics'02*, Svratka.
- Pásek M., Christé G., Šimurda J. (2003) Quantitative modelling of effect of transverse-axial tubular system on electrical activity of cardiac cells: development of model II, in: *CD of the Conference Engineering Mechanics'03*, Svratka.
- Satoh, H., Delbridge, L.M., Blatter, L.A., Bers, D.M. (1996) Surface:volume relationship in cardiac myocytes studied with confocal microscopy and membrane capacitance measurements: species-dependence and developmental effects. *Biophys. J.*, 70, pp. 1494-1504.
- Soeller C., Cannell M. B. (1999) Examination of the transverse tubular system in living cardiac rat myocytes by 2-photon microscopy and digital image-processing techniques. *Circ. Res.*, 84, pp. 266-275.
- Vornanen, M. (1992) Force-frequency relationship, contraction duration and recirculating fraction of calcium in postnatally developing rat heart ventricles: correlation with heart rate. *Acta Physiol. Scand.*, 145, pp. 311-321.
- Winslow, R.L., Rice, J., Jafri, S., Marban, E., O'Rourke, B. (1999) Mechanisms of altered excitation-contraction coupling in canine tachycardia-induced heart failure, II: model studies. *Circ. Res.*, 84, pp. 571-586.
- Yang, Z., Pascarel, C., Steele, D. S., Komukai, K., Brette, F., Orchard, C.H. (2002) Na^{+} - Ca^{2+} exchange activity is localized in the T-tubules of rat ventricular myocytes. *Circ. Res.*, 91, pp. 315-322.
- Yao, A., Spitzer, K.W., Ito, N., Zaniboni, M., Lorell, B.H., Barry, W.H. (1997) The restriction of diffusion of cations at the external surface of cardiac myocytes varies between species. *Cell Calcium*, 22, pp. 431-438.